Calcium based ternary nitrate salts for concentrating solar power applications

P Gandhre[1], V Shrotri[2] and L Muhmood[3]

1. Research Scholar, K J Somaiya College of Engineering, Somaiya Vidyavihar University, Mumbai Maharashtra 400077, India. Email: pranjal.gandhre@somaiya.edu
2. Project Engineer, C-DAC, Kolkata, West Bengal 700091, India. Email: varunshrotri59@gmail.com
3. Professor, K J Somaiya College of Engineering, Somaiya Vidyavihar University, Mumbai Maharashtra 400077, India. Email: luckman@somaiya.edu

ABSTRACT

The current work deals with the measurement of some thermophysical properties of $Ca(NO_3)_2$ based ternary nitrate molten salts as HTF (heat transfer fluid) / TES (Thermal Energy Storage) material for CSP (Concentrating solar power) plants. The density and viscosity of different compositions of the ternary salt mixture containing $Ca(NO_3)_2$, $NaNO_3$ and KNO_3 close to the liquidus has been experimentally measured. An attempt has also been made to measure the melting point of the salt using the cooling curve technique as well as Differential Scanning Calorimetry (DSC). Thermogravimetric analysis has also been performed to estimate the peak operating temperature of the salt. Compatibility of suitable pipe material (SS304) with molten salt has also been discussed. The salt mixture proves to be a viable alternative to the already existing HTFs like Therminol VP-1 (organic oil) or Solar Salt® in regards to its lower melting point, wider operating range, low cost, non-toxicity, sufficiently high density and comparable viscosity.

INTRODUCTION

With the increasing interest in sustainable power production and the need to reduce CO_2 emissions, renewable energy sources are becoming an important element of today's world energy balance. Among the current options of renewable energy, the Concentrating Solar Power (CSP) technologies *viz*: parabolic trough, linear fresnel reflector, parabolic dish and central tower, are gaining importance. In solar concentrator plants, the heat from the solar irradiance is transferred to a heat transfer fluid. A more popular method of transferring heat to the water is to transfer it to a fluid with higher thermal conductivity and heat storage capacity than water. This allows for more heat to be transferred to the working fluid.

Molten salts, namely fluoride salts, have been widely used in nuclear powerplants for heat transfer decades earlier than their use in CSP (Vignarooban *et al*, 2015; Rosenthal, 2010. It is only in the past four decades that molten salts have been used as heat transfer fluids in CSP to improve their effectiveness. Molten salts stand apart as a unique class of fluids that provide various advantages over their organic counterparts. Many of the salt mixtures developed and/or proposed for CSP applications are based on molten alkali nitrates. These mixtures make excellent HTFs (Heat Transfer Fluids) due to their lower viscosity, high volumetric heat capacity, and compatibility with the environment, high operating and decomposition temperature. Another important advantage of using molten salts is that they can also be used as a thermal energy storage medium. However, few thermophysical property data exist for promising ternary and quaternary salt mixtures as compared to simple binary mixture like 'Solar Salt®' containing 60 per cent $NaNO_3$ and 40 per cent KNO_3.

A poising problem with Solar Salt® is their high freezing point. This is not an issue during the diurnal operation, but when the temperature drops at night, special care must be taken to keep the salt from freezing. Auxiliary heaters are provided to keep this from happening, but the problem remains nonetheless. Hence, for solar thermal power to be cost-effective as a base load generation plant, the cost and efficiency of the plant must be improved. One possibility is by reducing the melting point of the heat transfer fluid, hence increasing the plant operation time. Currently, the most widely used molten salt HTF, the Solar Salt®, melts at 223°C (Vignarooban *et al*, 2015).

Classification of HTFs

HTF is one of the most important components for overall performance and efficiency of CSP systems. Since HTF is required in large quantities to operate a CSP plant, it is necessary to minimise the cost of HTF while maximising its performance. Besides transferring heat from the receiver to steam generator, hot HTF can also be stored in an insulated tank for power generation during periods of low solar insolation and at off-peak hours. Desired characteristics of an HTF include: low melting point, high boiling point and thermal stability, low vapour pressure (<1 atm) at high temperature, low corrosion with metal alloys used to contain the HTF, low viscosity, high thermal conductivity, high heat capacity for energy storage and low cost (Vignarooban *et al*, 2015; Srivastva, Malhotra and Kaushik, 2017).

Thermal oils can be either of petroleum origin or artificially synthesised in laboratories. These oils have a low freezing point. Most of these oils can be operated within a temperature range from 120°C to 280°C. Some of the thermal oils like Slytherm^{TM} 800 have a peak temperature of 400°C, but costs more than other HTFs like air, steam and molten salts (Ouagued, Khellaf and Loukarfi, 2013). Using air as HTF, an extensive temperature range can be obtained as there are no temperature limits for its use under practical applications. A major disadvantage of using air is the low thermal capacity and heat transfer rate between the fluid and the surfaces of the pipelines, so high pressure and high fluid velocities must be maintained. Liquid metals have only been tested for their use in CSP plants but have not been used for commercial CSP applications even though they have promising properties as HTF like excellent heat conductivity, low viscosity and a wide operating range (Boerema *et al*, 2012). Their practical applications in CSP have been limited as liquid metals like Sodium are highly reactive when in contact with air or moisture, while the lead-bismuth eutectic mixture is toxic in nature and prohibitively expensive even though it has the highest peak temperature of 1500°C (Pacio *et al*, 2013). Table 1 lists the key characteristics of some of the HTFs used in the industry.

Molten salts are regarded as the ideal materials for use in solar powerplants because of their excellent thermal stability under high temperatures, low vapour pressure, low viscosity, non-flammability and non-toxicity (Tian and Zhao, 2013). The increasing use of Solar Salt® as HTF and thermal energy storage medium even with its obvious limitations like high melting point and low operating range potentially creates the possibility to research for modified/new molten salts which could possibly replace the existing salt. Adding a third alkali nitrate to a binary salt mixture like Solar Salt® could have a positive effect on the thermophysical properties of the salt like, reducing its melting point, reducing its viscosity, increase in density and specific heat capacity and or improving the thermal stability of the salt at higher temperatures (Chen and Zhao, 2017). The properties of a ternary salt can in some cases be further improved by adding a fourth alkali nitrate; although at this point cost considerations comes into the picture.

Thermophysical properties have a huge impact on systems like heat exchangers and collector design in a powerplant. Viscosity is an important transport property having major implications on the economics and design of plant equipment's like pumps and heat exchangers. Density is needed for system sizing calculations as well as being a constituent of many dimensionless groups used for heat transfer and fluid flow calculations. Specific heat capacity is a very important heat transport property of an HTF having a major impact on selection of heat transfer components such as pipelines, heat exchangers and solar receiver lengths of a solar CSP plant. By using molten salts, the solar field output temperature can be increased to 450–500°C, thereby increasing the Rankine cycle efficiency of the power block steam turbine in the 40 per cent range as compared to 37.5 per cent for oil HTFs (Kearney *et al*, 2004). In addition to the thermal properties, other properties such as corrosivity have to be considered. Low or no corrosivity is desired to ensure safe and efficient usage and storage of the heat transfer fluid to the maximum lifetime possible of the system.

Table 2 compares the physical and thermal properties of the molten salt HTFs being used or under study. The binary eutectic salts like Solar Salt® has the highest melting point, at 223°C, compared to the group of eutectic salts mentioned in the table. A higher melting point would naturally reduce the operating range and working time and will also increase the start-up time. Reducing the melting point of the fluid has been one of the motivations of this study.

TABLE 1

Thermophysical properties of some heat transfer fluids in use.

	Therminol VP-I (@ 400°C) [a]	Dow-Corning 550® (@ 100°C) [b]	Xceltherm® 600 (@ 200°C) [c]	Air (@ 600°C) [d]	Water/steam (@ 600°C) [d]	Solar Salt® (@ 400°C) [e]	HITEC® (@ 400°C) [f]	HITEC XL® (300–400°C) [e,g]	Liquid Na (@ 550°C) [d,e]	Pb-Bi (@ 450°C) [h]
Density (g/cm^3)	0.649	1.098	0.53	0.0004565	0.000211	1.84	1.87	1.455	0.82	10.13
Viscosity (cP)	0.146	18.21	2.73	0.0025	0.028	1.7	2.8	12	0.23	1.44
Specific heat (kJ/kg-K)	2.62	1.615	2.24	1.023	2.42	2.66	1.32	1.15	1.25	0.143
Thermal conductivity (W/m-K)	0.0756	0.13	0.13	0.03779	0.08	0.55	0.57	0.52	62	13.7
Freezing point (°C)	12	-50	N/A	-	0	232	142	120	97	125
Decomposition temperature (°C)	400	315	315	-	-	600	535	550	883	1670
Remarks	These oils have a low freezing point. Most operate safely within a temperature range of 120°C to 280°C.			It does not freeze under practical application temperatures, does not boil and is inert by nature. It has poor heat transport properties, very low heat capacity and has containment issues	Preferred fluid for low temperature solar collectors' applications. It has high specific heat and is easy to pump due to having very low viscosity. Although, high pressure and high velocity must be maintained for steam.	They have a high freezing point and can be used up to 500°C. Molten salts also have low vapour pressure and are economical. They can also be used as a thermal energy storage medium.			Liquid metals have excellent heat transfer properties and a very high operating temperature range. However, liquid metals and their alloys can be volatile, toxic, corrosive and very expensive.	

NB: [a] – Eastman Chemical Company (2019); [b] – Dow Chemical Company (2017); [c] – Radco Industries (2024); [d] – Vignarooban *et al* (2015); [e] – Sohal *et al* (2010); [f] – Coastal Chemical Co. LLC (2024); [g] – Fernández *et al* (2014); [h] – Pacio *et al* (2013).

TABLE 2

Thermophysical properties of some existing alkali nitrate salt mixtures.

	Solar Salt® (KNO_3-$NaNO_3$) [a,b]	**Hitec® (KNO_3-$NaNO_3$-$NaNO_2$)** [b,c]	**Hitec XL® (KNO_3-$NaNO_3$-$Ca(NO_3)_2$)** [d,e]	**$NaNO_3$-KNO_3-$LiNO_3$** [f,g,h,i]	**KNO_3-$LiNO_3$-$Ca(NO_3)_2$** [e,j]	**$NaNO_3$-KNO_3-$CsNO_3$** [k]	**$NaNO_3$-KNO_3-$LiNO_3$-$Ca(NO_3)_2$** [l]	**$NaNO_3$-KNO_3-$LiNO_3$-$CsNO_3$-$Ca(NO_3)_2$** [m]
Composition (wt%)	60/40	50/7/43	48/16/36	28/52/20	65/10/25	20/24/56	12/40/21/27	7/21/7/41/25
Density (g/cm^3)	1.83 @ 300°C	1.86 @ 300°C	1.93 @ 300°C	1.97 @ 140°C	N/A	2.4 @ 200°C	N/A	N/A
Viscosity (cP)	3.26 @ 300°C	3.16 @ 300°C	6.3 @ 300°C	3 @ 300°C	2 @ 300°C	9.5 @ 200°C	5 @ 300°C	N/A
Specific heat (kJ/kg-K)	1.1 @ 400°C	1.56 @ 300°C	1.45 @ 300°C	N/A	1.395 @ 390°C	1.18 @ 300°C	N/A	1.22 @ 150°C
Thermal conductivity (W/m-K)	0.55	0.605	3.25	N/A	0.1	N/A	N/A	N/A
Melting point (°C)	232	142	120	121	~100	152	95	65
Decomposition temperature (°C)	600	535	550	540	500-567	525	520	>500

NB: [a] – Sohal *et al* (2010); [b] – Serrano-López, Fradera and Cuesta-López (2013); [c] – Coastal Chemical Co. LLC (2024); [d] – Dow Chemical Company (2017); [e] – Fernández *et al* (2014); [f] – Olivares and Edwards (2013); [g] – Bradshaw (2009); [h] – Bradshaw (2010); [i] – Roget, Favotto and Rogez (2013); [j] – Zhao and Wu (2011); [k] – Zhang *et al* (2018a); [l] – Bradshaw and Siegel (2008); [m] – Jonemann (1979).

Table 3 lists the positive and negative effects of adding different cations to the existing binary mixture Solar Salt®. Adding suitable salts to a binary mixture can reduce the melting/freezing point of the mixture. Adding sodium nitrite to the Solar Salt® reduces the melting point to 142°C, while adding calcium nitrate or lithium nitrate will reduce the melting point to ~120°C. The addition of calcium nitrate to $NaNO_3$ and KNO_3 decreases the mixture freezing point to about 110°C, but also increases the viscosity of the mixture. A quaternary mixture such as the 'Sandia Mix' (Bradshaw and Siegel, 2008), containing sodium, potassium, calcium and lithium nitrate brings down the melting point to 95°C while adding caesium nitrate to the same forms a mixture of five salts, which has a melting point of 65°C (Jonemann, 1979). Although, the low melting point of a four or five component salt mixture appears appealing, the addition of lithium nitrate and or caesium nitrate increases the cost of the final product making it not economical.

TABLE 3

Effect of adding different cation(s) to $NaNO_3$-KNO_3 mixture on different properties of the heat transfer fluid.

	Ca^{2+}	Li^{+}	Cs^{+}	Li^{+}-Ca^{2+}	Li^{+}-Ca^{2+}-Cs^{+}
Melting point	+	+	+	+	+ +
Decomposition temperature	–	–	–	–	–
Density	+	–	+	0	0
Viscosity	–	0	0	0	0
Specific heat	0	0	+	0	0
Cost	+	–	–	–	– –

NB: '+' stands for a positive impact on the property, '–' means a negative impact while '0' means no significant change in property. '++'means the best and '- -'means the worst of various combinations.

The Solar Salt® and the ternary salt with calcium and lithium nitrate have a viscosity of 3–5 cP at around 300°C, while the Hitec® is at 3.6 cP at 300°C. The mixtures containing $Ca(NO_3)_2$ present viscosity values relatively high at 6 cP @ 300°C depending on the composition. The Sandia Mix quaternary salt has a viscosity of 2–3 cP at 400°C. The addition of calcium nitrate always results in a higher density and a glassy state at the melting point which increases its viscosity at lower temperatures (Chen and Zhao, 2017). However, calcium nitrate has the lowest cost among the alkali nitrates and adding it to the binary mix reduces the melting point of the HTF which increases the operating range and reduces the cost in freeze protection of the salt during off-peak hours (Kearney *et al*, 2003).

The thermophysical data of molten salts are not easily obtained due to the inherent difficulty in conducting experiments at elevated temperatures and the thermophysical data of other promising ternary salt mixtures such as the current composition in focus has not been reported to a similar extent. Any uncertainty in the thermophysical data of a fluid can have implications wherein the equipment design depending on those properties will be either under or over-designed. Therefore, it becomes imperative to choose the right HTF and equally important to have accurate data on the properties of the same to help in the design of a new HTF. The authors have thus attempted to measure the density, viscosity, melting point, corrosivity and thermal decomposition of one such salt mixture containing $Ca(NO_3)_2$, $NaNO_3$ and KNO_3.

MATERIALS AND METHODOLOGY

The salt mixtures (Composition 1 and 2 – see Table 4) were prepared using $Ca(NO_3)_2$, $NaNO_3$ and KNO_3, purchased from AB Enterprises, Mumbai, with a known purity of 99 per cent, while for Composition 3, the raw materials were purchased from Sigma Aldrich. The salts were pre-heated in a Muffle furnace at 220°C for at least six hours. To compare the results, Composition 3 was heated to 250°C under vacuum. Post-treatment of the salts: the weights of the individual salts were measured before and after heating them to measure the mass loss due to the evaporation of

moisture and chemically bound water in the salts. The salts were mixed according to the desired compositions after being finely grounded. Suitable weights of the salt mixtures were taken for density and viscosity measurements. The same quantity of salt was used for the cooling curve measurement (Composition 1) while 1 g of salt was used for the Thermogravimetric Analysis (TGA) experiment.

TABLE 4

Composition of the salt mixtures being tested.

	$Ca(NO_3)_2$ (wt%)	$NaNO_3$ (wt%)	KNO_3 (wt%)	Melting point (°C)
Composition 1	32	24	44	130 [a]
Composition 2	36	16	48	132 [b]
Composition 3	39	15	46	150

NB: [a] – Chen and Zhao (2017); [b] – Calvet et.al.(2013).

Melting point determination

A cooling curve provides a complete picture of the heat dissipation and cooling of a substance as a function of temperature. This test has been performed on the HITEC® salt (Figure 1), to determine the melting point of the salt for the purpose of process calibration. For the experiment, the salt was initially heated in a crucible to 300°C in a muffle furnace and allowed to melt completely. Once in liquid form, the molten salt is removed from the furnace and allowed to cool naturally while a thermocouple connected to a data logger logs the temperature readings continuously. The reduction in temperature of the salt is then graphically represented as a cooling curve. The nature of the curve – as the temperature reduces with time – is exponential, except for a certain portion where the temperature remains seemingly constant. This suggests that there is a change of state going on from liquid to solid.

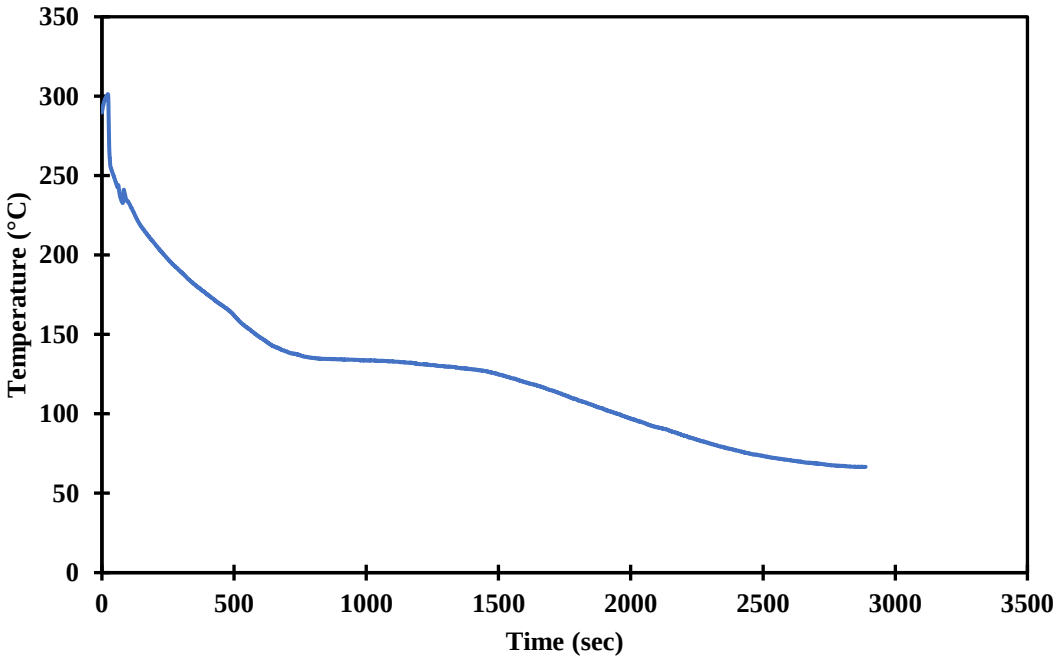

FIG 1 – Cooling curve test results for HITEC® salt.

The same technique was used to estimate the melting point of the ternary salt mixture. Differential Scanning Calorimetry (DSC) of the salt mixture was also used to confirm the same.

Density and viscosity measurement

The salt mixtures were melted on a hot plate to check for the presence of solids. It was observed that the liquid was clear and uniform at temperatures above the melting point. Measurements of both density as well as viscosity were performed after the sample attained its liquidus temperature. Brookfield DV-II viscometer and a bottom loaded Mettler-Toledo precision balance was used to measure the viscosity and density of the molten salts respectively. The rotating element used for viscosity measurement and the sinker for the density measurement is an SS304 bob and anSS304 crucible. SS304 was used for both the sinker and the crucible since it has been shown to have good corrosion resistance in the presence of nitrates at high temperatures under various atmospheric conditions and time periods (Zhai *et al*, 2017).

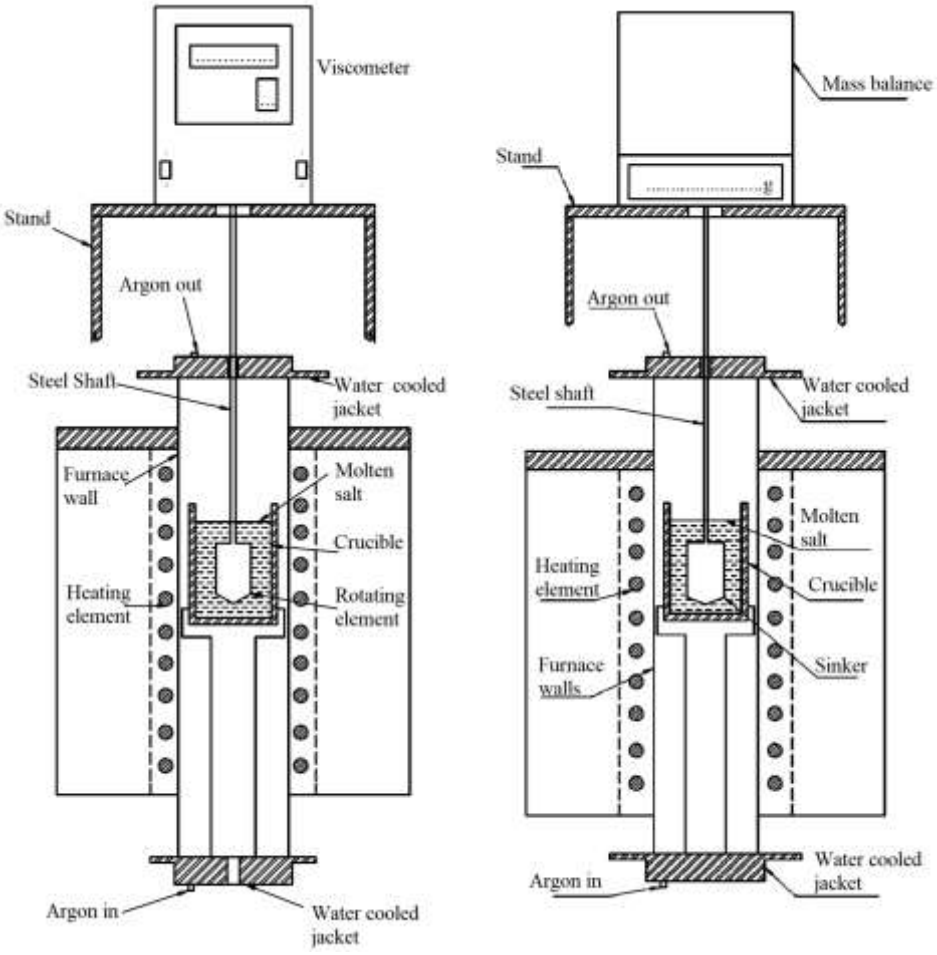

FIG 2 – Set-up for viscosity (left) and density (right) measurement.

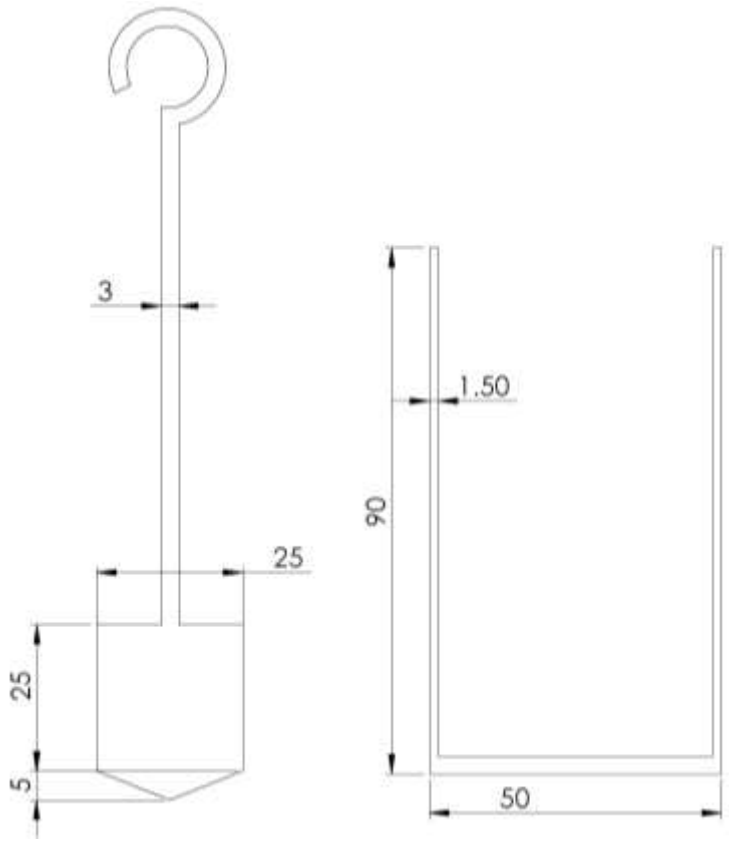

FIG 3 – (a) Rotating element/sinker; (b) Crucible used for density and viscosity measurement. All dimensions are in mm.

The viscosity measurements were performed using Brookfield DV-II (Figure 2), which measures the viscosity of a fluid by a rotational method in which the bob rotates in a crucible filled with the desired liquid. It measures the torque applied on the rotating element by the fluid due to the resistance to its rotation in the fluid (Zhang *et al,* 2018b). In order to obtain the necessary sensitivity to measure the low viscosity liquids the clearance between the stationary and rotating parts has to be made very small. The viscometer reading is first set to zero by using the 'auto zero' function on the front panel. The spindle is attached to the viscometer at this point and the motor is run at 12 rev/min. The display blinks ten times and the reading will settle to zero, indicating that the set-up is complete. The SS304 bob is attached to the spindle. The bob at this point is completely immersed in the liquid in the crucible. The motor is run, starting from the lowest rev/min reading for the % torque to be measured, which is shown on the display. Only % torque values between 10 and 90 per cent are considered as recommended by the viscometer manufacturer. The rev/min of the motor is progressively increased using the dial on the side of the viscometer and % torque for each rev/min is noted. The viscosity of the salt mixture is calculated using Equation 1 which is provided in the system manual of the viscometer.

$$\eta = \frac{100 \times \mathrm{TK} \times \mathrm{SMC} \times \mathrm{Y}}{\mathrm{rev/min}} \tag{1}$$

where:

TK is a system constant equal to 0.09373

SMC is a constant of the rotating element, measured using standard fluids of known viscosity

Y is the % torque read by the viscometer for a particular rotation speed

The density of the salt mixture is measured by using the Archimedean method (Figure 2), where a sinker is weighed before and after being immersed in the liquid. The reduced weight of the sinker after being immersed in the liquid is the consequence of the sinker being provided an upward force

on it due to the buoyancy of the fluid. The weight is measured using a bottom loaded Mettler-Toledo precision balance ME 204 with 0.0001 g accuracy.

The density of the salt mixture was measured between the temperatures of 190 and 462°C. The sinker was weighed before and after immersing it in the salt mixture, once beyond its melting point. The density of the salt mixture was then calculated using Equation 2 which accounts for the increase in volume of the steel sinker at elevated temperatures. Temperature was measured after allowing the system to attain equilibrium for 20 mins and then measuring the temperature using a K–type thermocouple.

$$\rho = \frac{\Delta m}{V \times [1+3 \times (\alpha \times (T - T_0))]} \quad (2)$$

where:

- ρ is the density of the salt sample
- Δm is the difference in the mass readings before and after being immersed in the molten salt
- V is the volume of the sinker that is immersed in the salt
- α is the thermal expansion coefficient of the sinker material
- T is the temperature of the salt in °C
- T_o is the ambient temperature in °C

Corrosion

Goods and Bradshaw (2004) reported corrosion rates of around 6–10 µm per annum for two different stainless-steel alloys (SS304 and SS316) immersed in HITEC XL® for 7008 hrs at 570°C. This suggests that the SS alloys could be acceptable candidates for use with HITEC XL® molten salt at temperatures up to 500°C.

For this experiment, the corrosion testing has been performed on SS304 by the salt with Composition 1. The specimens obtained as 26 × 28 × 2 mm SS304 strips, were cleaned thoroughly and dried before being immersed in the salt. The test was conducted as static immersion test, to obtain the data on corrosion. Each of the SS strips was weighed before the test in order to monitor the weight change. The exposure test was performed at 400°C in a muffle furnace with five samples immersed in five crucibles. Each sample was removed every 120 hours to measure the weight change. Microscopy can be employed to check the micro-structural changes in the metal due to its interaction with the salt. The following formula is used to calculate the corrosion rate (Trent, Goods and Bradshaw, 2016):

$$A = \frac{m_0 - m_1}{S} \quad (3)$$

where:

- A is the corrosion amount of metal (mg/mm^2)
- m_o is specimen quality before test (mg)
- m_1 is specimen quality after test (mg)
- S is the total surface area of the specimens (mm^2)

Thermogravimetric analysis

Cordaro, Rubin and Bradshaw (2011) had observed that the nitrate salt decomposed to nitrite at high temperatures in a reversible manner. This is followed by the nitrite decomposing to metal oxides, nitrogen oxide and other gases (Mohammad, Brooks and Rhamdhani, 2017). Thermogravimetric analysis was performed on the salt (Composition 1) to evaluate the thermal stability of the material at high temperatures. The mass of the sample is measured over time as the temperature increases. This provides the data about the changes in the mass of the sample due to phase changes, absorption, desorption and thermal decomposition. For a particular temperature range, there will be no observable mass change in the sample. Loss of moisture from the sample

usually corresponds to a negligible mass loss, while beyond a certain temperature will gradually increase to drastic proportions as the material begins to degrade. This will indicate the upper temperature limit for the material.

Initially, the TGA test was carried out using an empty SS304 crucible to determine the change in mass occurring for the crucible alone. This will help in accounting for the mass loss from the crucible occurring during the actual experiment. The crucible was connected to a bottom loaded Mettler-Toledo precision balance mounted above a vertical furnace using a SS304 wire. The mass balance was connected to a computer which logged the readings to an Excel sheet at a specific rate. The temperature was recorded using a thermocouple connected to a data logger to record the readings.

After the experiment was performed on the blank, it was repeated for the salt sample. The crucible was loaded with 1 g of salt (Composition 1) and the crucible was underneath the balance using a SS304 wire. The heating rate of the furnace was kept low, at 3°C/min and an inert atmosphere of argon was maintained inside the furnace. The mass readings were recorded up to a temperature of 600°C.

RESULTS AND DISCUSSION

Density and viscosity

Density and viscosity variations with temperature for both compositions were measured and are shown in Figures 4 and 5 respectively.

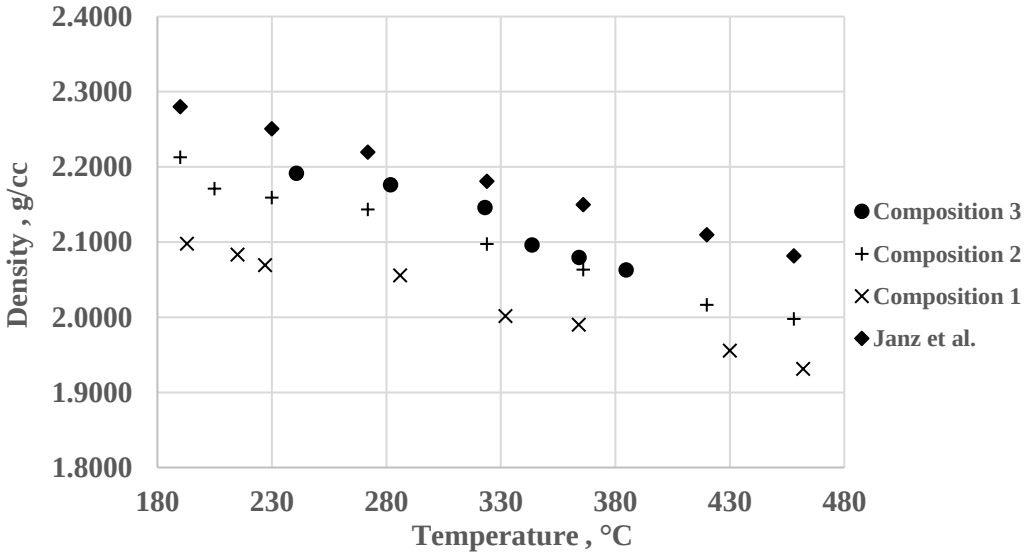

FIG 4 – Density temperature relations for Compositions 1, 2 and 3. The density of Composition 2 was also compared with (Janz, 1998).

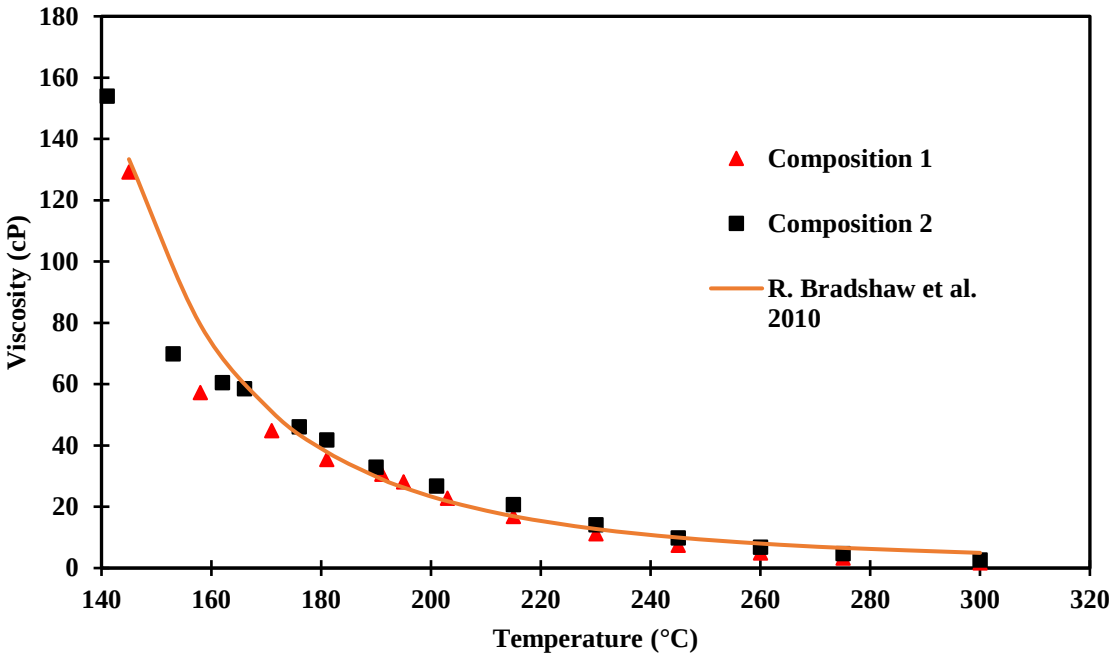

FIG 5 – Viscosity temperature relations for Compositions 1 and 2.

The density of the compositions was measured between 190°C and 462°C and is reported in Figure 4. The density of both the compositions is found to decrease linearly with temperature, with Composition 2 showing a slightly higher density. Composition 2 has 4 per cent more calcium nitrate which results in higher density and is consistent with the literature data reported by Bradshaw (2009) and Zhang *et al* (2018b) for other calcium nitrate-based salt systems. Upon repeating the measurements for the same composition an average error of ±2 per cent was obtained. The densities measured of the compositions are correlated to the density of the similar salt mixtures obtained from the volumetric additive rule using the Equation 5:

$$\rho = \frac{\sum X_i \times MW_i}{\sum V_i} \tag{4}$$

$$and\ V_i = A_v + B_v \times T \tag{5}$$

The constants A_v and B_v were referred from Bradshaw (2009). The deviation in the measured and estimated values (additive rule) was very close with an error less than 5 per cent for the measured temperature range.

The viscosity of the salt mixture Compositions 1 and 2 was observed to be decreasing exponentially. The results of the experiment are plotted in Figure 5. The viscosity of the compositions beyond 203°C is extrapolated from the previous values as the temperature of the crucible could not be raised any further due to extremely low viscosity which could be measured by the viscometer. The viscosity of the compositions varied from 154 cP at 141°C to less than 11 cP beyond 230°C. The high viscosity of the compositions near the melting point is known to be due to the presence of calcium nitrate in the mixture as has been observed by Bradshaw and Siegel (2008). This trend can also be observed in the experimental data as Composition 2 having more viscosity than Composition 1. This would mean that the temperature of the collector loop in a CSP plant to be near or above 200°C in order to reduce the pumping power required. The viscosity of Composition 2 has been correlated with the viscosity-temperature relation obtained by fitting a curve in the experimental data reported by Bradshaw (2010) whose ternary salt system has the same composition. An average error of 17 per cent was obtained and on repeating the experiments, a deviation of less than ±2 per cent was obtained. The viscosity data for Composition 1 could not be found in the literature implying that it may not have been measured yet. It has been successfully applied by the authors to predict the density and viscosity of $LiNO_3$ and $CsNO_3$ based ternary alkali nitrate salt systems (Shrotri and Muhmood, 2020) and further details of the model and its correlation to the current salt composition can be referred to elsewhere.

Melting point

A sharp cooling could not be replicated to obtain the melting point (Figure 6). However, a change in slope can be observed at two points *viz*, 145°C and 115°C which suggests that the liquid freezes within this temperature range. This is likely due to the melting point of the pure salts in the mixture being dissimilar. The melting points of sodium nitrate, potassium nitrate and calcium nitrate are 308°C, 334°C and 561°C respectively and hence the mixture freezes at a uniform rate as the pure components solidify at different time.

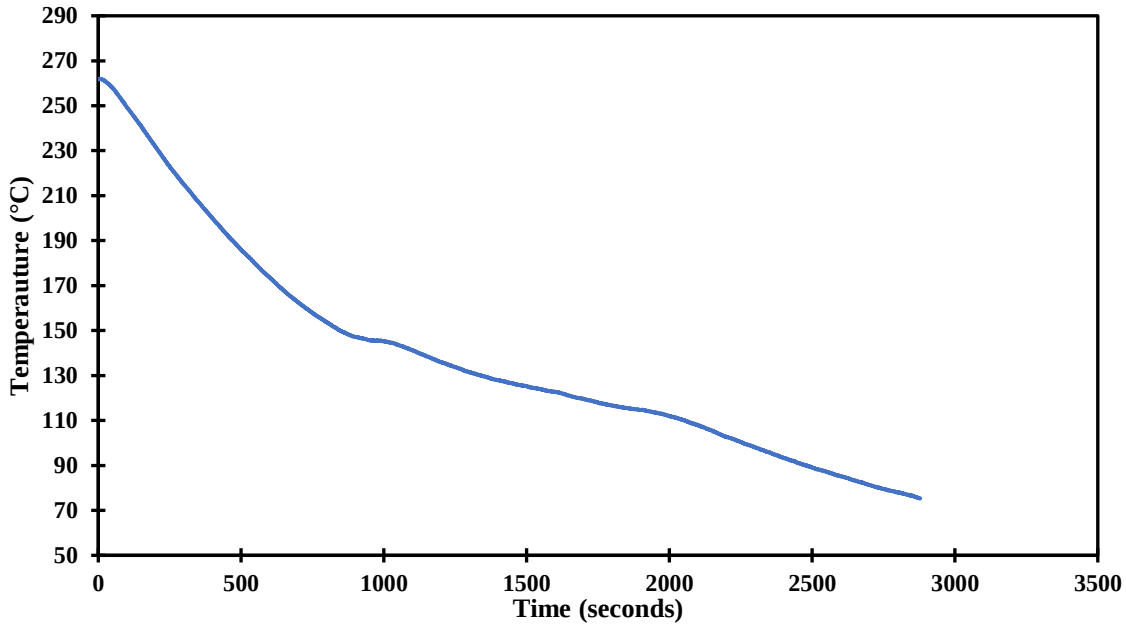

FIG 6 – Cooling curve test results for Composition 2.

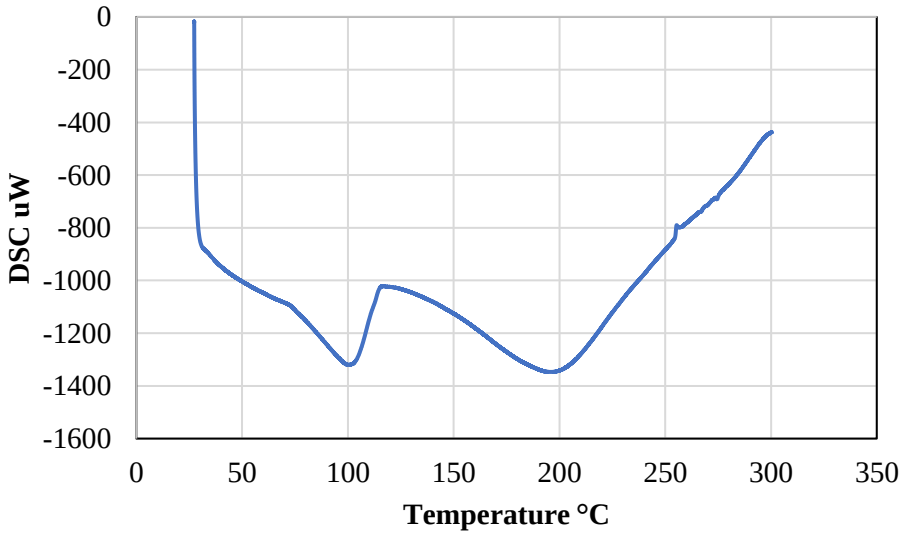

FIG 7 – Differential Scanning Calorimetry (DSC) of Composition 2.

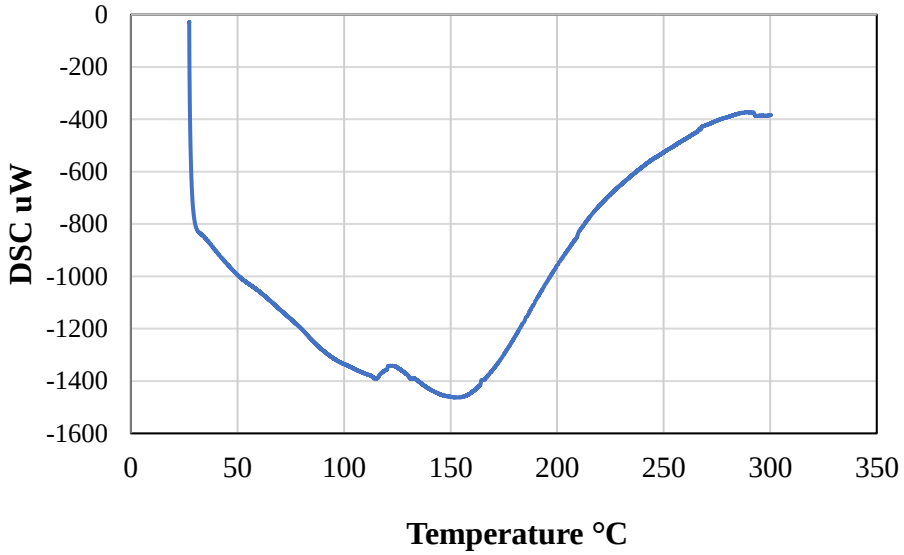

FIG 8 – Differential Scanning Calorimetry (DSC) of Composition 3.

Differential Scanning Calorimetry (DSC) was carried out for Compositions 2 and 3 (figure 7 and figure 8) in order to obtain a better understanding of the melting range. It can be seen that in both these samples, there is a range of temperature where the melting starts and ends. For Composition 2, it is between 108°C and 180°C and for Composition 3 showed melting between 112°C and 155°C.

Corrosion

Coupons of 26 × 28 × 2 mm dimensions were machined from SS304 to ensure complete immersion in the salt mixture as per the standard guidelines for evaluating corrosion (ASTM G1–03; ANSI, 2003). After the experiment, descaling is required to remove the corrosion products and the weight loss of the coupon was measured. The following methodology was used to estimate the corrosion rate.

The increase in weight of the sample was assumed to be due to the oxidation of Fe to Fe_2O_3 and could be calculated by finding the weight gained after through washing the coupon with warm water. The amount of Fe corroded can be calculated as follows:

$$\mathrm{m_{Fe}/time} = \frac{\mathrm{m_1 - m_0}}{wt.of\ Fe\ in\ the\ oxidation\ product} \tag{6}$$

$$\mathrm{m_{loss}/area/time} = \frac{\mathrm{m_{Fe}}}{\mathrm{A_s}} \tag{7}$$

$$\mathrm{t_{loss}/time} = \frac{\mathrm{m_{loss}/time}}{\rho} \tag{8}$$

where:

- mF_e is the weight loss due to oxidation
- A_s is the surface area of the sample
- t_{loss} is the thickness loss due to the oxidation of iron on the surface
- ρ is the density of the oxidation product (5.24 g/cc)

The experimental data is provided in Table 5 and Figure 9. Extrapolating the results based on the data yields a total corrosion rate of 2.58 µm/a for the current salt mixture (Composition 1).

TABLE 5

Corrosion in the SS304 sample in ternary molten salt (Composition 1).

Time (hrs)	Initial weight, m_0 (gm)	Final weight, m_1 (gm)	Net weight increase (m_1-m_0) (mg)	A_s (cm^2)	mF_e (mg/a)	wt loss/ area ($g/cm^2/a$)	t_{loss}/time (µm/a)
120	9.5678	9.5678	0	1.482	0.0000	0.0000	0.0000
240	9.6185	9.6187	0.2	1.482	0.0009	0.0006	0.0758
360	9.6285	9.6291	0.6	1.456	0.0027	0.0018	0.2273
504	9.6514	9.6525	1.1	1.508	0.0049	0.0033	0.4168
624	9.5502	9.5519	1.7	1.456	0.0076	0.0052	0.6441

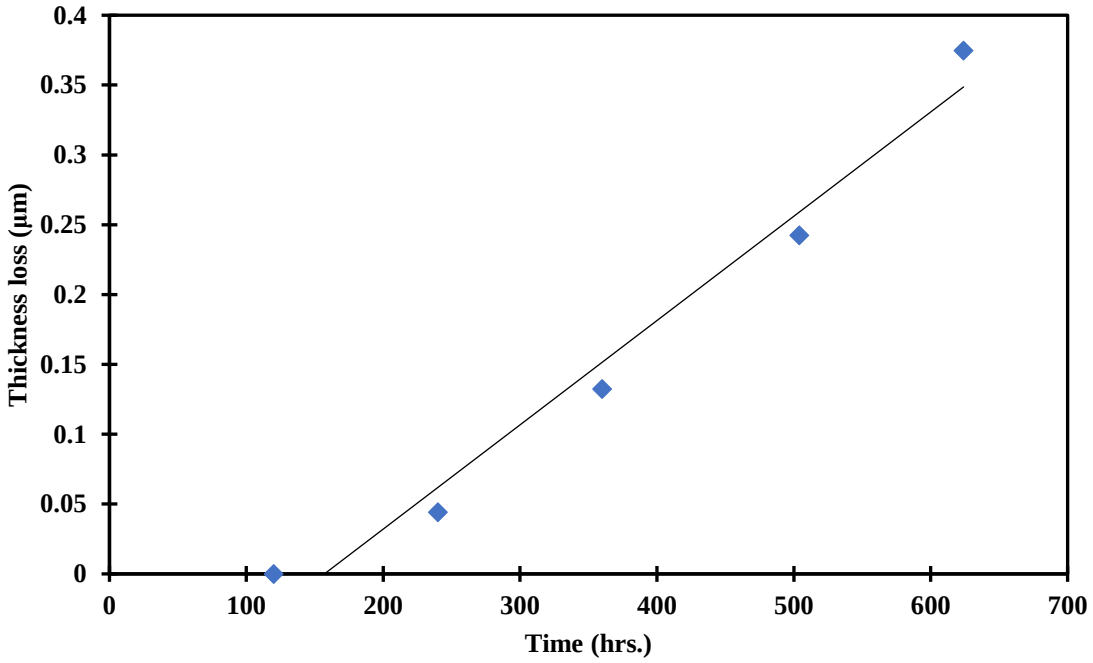

FIG 9– Corrosion rate for SS304 at 400°C.

Thermogravimetric analysis

The TGA was performed on the salt sample (Composition 1) as well as the blank crucible in order to account for any mass change in the crucible. Both the tests were performed up to 600°C with a heating rate of 10°C/min in an inert atmosphere of argon.

The result is shown in Figure 8 and it is observed that apart from a slight weight loss (1 per cent) due to chemically bound water release, the salt showed no significant change up to 600°C. Beyond this point the weight loss of the salt reduced below 98 per cent of the initial weight. However, the weight loss increased drastically after 600°C. This consistent with the findings in the literature, where the maximum temperature of the ternary salt system of a similar composition was reported to be 550°C.

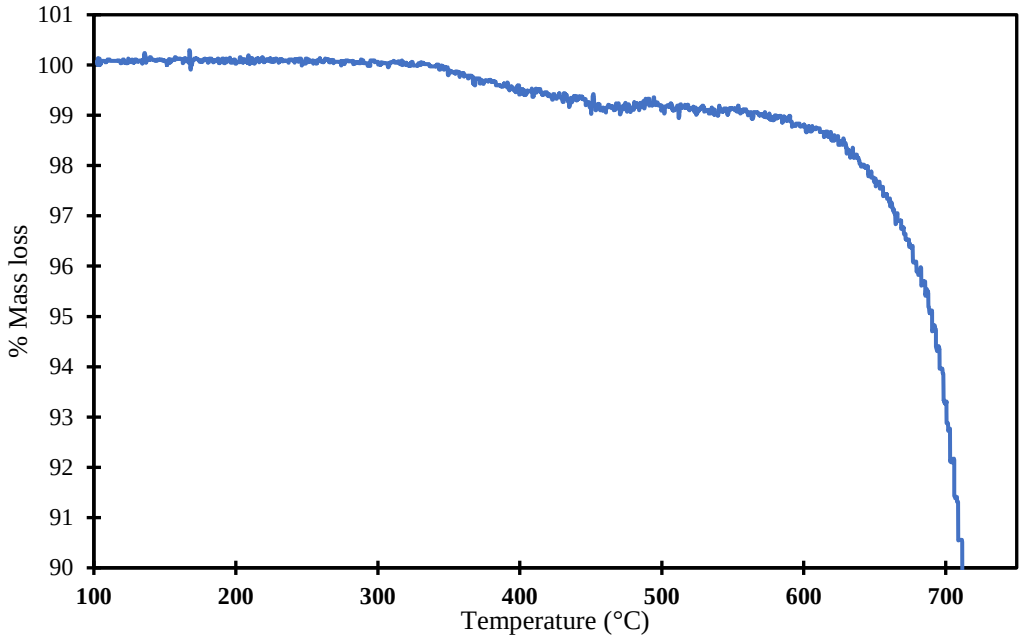

FIG 10– TGA curve for the ternary salt sample.

Comparison to existing molten salt HTFs

TABLE 6

Thermophysical properties of Solar Salt® compared with the new ternary salt.

	Solar Salt®	**$Ca(NO_3)_2$–$NaNO_3$–KNO_3**	**Hitec®**
Density (g/cc)	1.84 @ 400°C	1.93 @ 400°C	1.87 @ 400°C
Viscosity (cP)	3.2 @ 300°C	4.9 @ 300°C	3.16 @ 300°C
Corrosivity on SS304 (µm/a)	6–10 @ 570°C [a]	2.58 @ 400°C	N/A
Melting point (°C)	223	~130	142
Decomposition temperature (°C)	600	~ 600	535

NB: [a] – Goods and Bradshaw (2004).

The binary eutectic salts like Solar Salt® has the highest melting point, at 223°C (Table 6), compared to the group of eutectic salts mentioned in Table 2. A higher melting point would naturally reduce the operating range and working time and will also increase the start-up time. Adding another salt to a binary mixture has the effect of reducing the melting point of the mixture, like adding calcium nitrate reduced the melting point to around 130°C and the ternary salt mixture Hitec® which has a melting point of 142°C. The peak operating temperature limit of the salt.

Due to the presence of calcium nitrate in the salt system, the density of the salt has increased by 5 per cent. A higher density and specific heat would imply that the heat transfer fluid has a higher volumetric heat storage capacity. The viscosity of molten salts as this property strongly affects pumping costs, among other aspects of system performance. It is an important transport property having major implications on the economics and design of plant equipment's like pumps and heat exchangers. The mixtures containing $Ca(NO_3)_2$ exhibit relatively high viscosity. However, the viscosity of the salt reduces to a comparable value to the Solar Salt® at higher temperatures.

Stainless steel alloys have been suggested to an acceptable candidate for use with nitrate salts. The corrosion test was performed of SS304 specimens for 620 hours at 400°C. The experimental data was extrapolated to yield a total corrosion rate of 2.58 µm/a. This corrosion is compared to the

corrosion rate of 6–10 µm/a. of the Solar Salt® (Goods and Bradshaw, 2004) however at a higher temperature.

The maximum temperature of the salt was found to be at 600°C using TGA, which is comparable to the Solar Salt® which has a maximum temperature of 565°C. Coupled with a lower melting point the operating temperature range for this salt is increased leading to a lower cost of freeze protection of the salt. It should also be noted that adding calcium nitrate also reduces the materials cost as it is the cheapest of the alkali nitrates used for the mixtures mentioned in this study (Kearney *et al*, 2003).

CONCLUSION

It was observed from experiments that the addition of calcium nitrate to the binary nitrate salt mixture resulted in a lowering of the melting point of the system from 223°C to 130°C. A commonality between Compositions 1, 2 and 3 is their relatively high density and viscosity, which is mainly attributed to the presence of calcium nitrate. Moreover, both the properties were observed to increase proportionally with the increase in the amount of calcium nitrate present in the ternary system. This is supported by the data observed in the literature. Although calcium nitrate causes a relative increase in the viscosity of the salt system, the viscosity eventually decreases beyond the temperature of 200°C to pose no hindrance in its use as HTF. This ternary salt mixture has a relatively high density of around 2 g/cc and is cheaper than the organic oils being used currently. It would therefore offset any increase in the cost of the system resulting from upgrading the heat transfer loop.

Static immersion tests performed on SS304 suggest stainless steel alloys to be a potential metal for use with nitrate salts as they appear to be more resistant to corrosion due to nitrates. The peak operating temperature of the salt was found to be comparable to the Solar Salt® which has a maximum temperature of 600°C. Since the minimum operating temperature is also reduced, the cost in freeze protection of the salt also gets reduced while maintaining high temperature efficiency. The properties measured in this study can further be modified by changing the composition and or the components of the system to obtain the optimum balance between cost and efficiency. The result of such projects would imply a possible alternative to the already existing molten salt HTF Solar Salt® and would open doors to assess its long-term performance for its application in concentrating solar powerplants.

ACKNOWLEDGEMENT

The authors would like to acknowledge the Department of Science and Technology (SERB/EMR/2016/002784) and (SERB/CRG/2022/001796) for funding the project.

REFERENCES

American National Standards (ANSI), 2003. ASTM G1–03 – Standard Practice for Preparing, Cleaning, and Evaluating Corrosion Test Specimens, December 2003.

Boerema, N, Morrison, G, Taylor, R and Rosengarten, G, 2012. Liquid sodium versus Hitec as a heat transfer fluid in solar thermal central receiver systems, *Solar Energy*, 86:2293–2305. https://doi.org/10.1016/j.solener.2012.05.001

Bradshaw, R W, 2009. Sandia report effect of composition on the density of multi-component molten nitrate salts. Sandia National Laboratories Report SAND2009-8221 Available at: https://doi.org/10.2172/983681

Bradshaw, R W, 2010. Sandia report viscosity of multi-component molten nitrate salts-liquidus to 200°C. Sandia National Laboratories Report SAND2010-1129 Available from: https://doi.org/10.2172/983680

Bradshaw, R W and Siegel, N P, 2008. Molten nitrate salt development for thermal energy storage in parabolic trough solar power systems. In Proceedings of the second International Conference on Energy Sustainability 2008, ES 2008. V. 2. doi.org/10.1115/ES2008-54174.

Calvet, N, Gomez, JC, Faik, A, Roddatis, V V., Meffre, A, Glatzmaier, GC, Doppiu, S & Py, X. 2013. Compatibility of a post-industrial ceramic with nitrate molten salts for use as filler material in a thermocline storage system. *Applied Energy*. 109:387–393. doi.org/10.1016/j.apenergy.2012.12.078

Chen, Y Y and Zhao, C Y, 2017. Thermophysical properties of Ca(NO3)2-NaNO3-KNO3 mixtures for heat transfer and thermal storage, *Solar Energy*, 146:172–179. https://doi.org/10.1016/j.solener.2017.02.033

Coastal Chemical Co. LLC, 2024. HITEC heat transfer salt [online]. Available from: https://coastalchem.com/products/heat-transfer-fluids/hitec-heat-transfer-salt/ (Accessed: 20 January 2024).

Cordaro, J G, Rubin, N C and Bradshaw, R W, 2011. Multicomponent molten salt mixtures based on nitrate/nitrite anions, *Journal of Solar Energy Engineering, Transactions of the ASME*, 133. https://doi.org/10.1115/1.4003418

Dow Chemical Company, 2017. DOWSIL TM 550 Fluid features and benefits. www.dow.com/en-us/document-viewer.html?docPath=/content/dam/dcc/documents/22/22-0071-01-dowsil-550-fluid.pdf

Eastman Chemical Company, 2019. Therminol® VP-1 Technical Bulletin Report. https://productcatalog.eastman.com/tds/ProdDatasheet.aspx?product=71093459&pn=Therminol+VP-1+Heat+Transfer+Fluid#_ga=2.100194838.961084841.1716276248-1262082965.1716276248

Fernández, A G, Ushak, S, Galleguillos, H and Pérez, F J, 2014. Development of new molten salts with LiNO3 and Ca(NO3)2 for energy storage in CSP plants, *Appl Energy*, 119:131–140. https://doi.org/10.1016/j.apenergy.2013.12.061

Goods, S H and Bradshaw, R W, 2004. Corrosion of stainless steels and carbon steel by molten mixtures of commercial nitrate salts, *J Mater Eng Perform*, 13:78–87. https://doi.org/10.1361/10599490417542

Janz, G, 1988. Thermodynamic and transport properties for molten salts: Correlation equations for critically evaluated density, surface tension, electrical conductance and viscosity data, *J Phys Chem Ref Data*, 17.

Jonemann, M, 1979. Advanced Thermal Storage System with Novel Molten Salt, NREL/SR-5200–58595.

Kearney, D, Herrmann, U, Nava, P, Kelly, B, Mahoney, R, Pacheco, J, Cable, R, Potrovitza, N, Blake, D and Price, H, 2003. Assessment of a molten salt heat transfer fluid in a parabolic trough solar field, *Journal of Solar Energy Engineering, Transactions of the ASME*, 125:170–176. https://doi.org/10.1115/1.1565087

Kearney, D, Kelly, B, Herrmann, U, Cable, R, Pacheco, J, Mahoney, R, Price, H, Blake, D, Nava, P and Potrovitza, N, 2004. Engineering aspects of a molten salt heat transfer fluid in a trough solar field, *Energy*, 29:861–870. https://doi.org/10.1016/S0360-5442(03)00191-9

Mohammad, M, Bin, Brooks, G A and Rhamdhani, M A, 2017. Thermal analysis of molten ternary lithium-sodium-potassium nitrates, *Renew Energy*, 104:76–87. https://doi.org/10.1016/j.renene.2016.12.015

Olivares, R I and Edwards, W, 2013. LiNO3–NaNO3–KNO3 salt for thermal energy storage: Thermal stability evaluation in different atmospheres, *Thermochim Acta*, 560:34–42. https://doi.org/10.1016/j.tca.2013.02.029

Ouagued, M, Khellaf, A and Loukarfi, L, 2013. Estimation of the temperature, heat gain and heat loss by solar parabolic trough collector under Algerian climate using different thermal oils, *Energy Convers Manag*, 75:191–201. https://doi.org/10.1016/j.enconman.2013.06.011

Pacio, J, Singer, C, Wetzel, T and Uhlig, R, 2013. Thermodynamic evaluation of liquid metals as heat transfer fluids in concentrated solar power plants, *Appl Therm Eng*, 60:295–302. https://doi.org/10.1016/j.applthermaleng.2013.07.010

Radco Industries, 2018. XCELTHERM® 600 – Engineering Properties. Available from: https://www.radcoind.com/fluid/xceltherm-600/ [Accessed 20 January 2023].

Roget, F, Favotto, C and Rogez, J, 2013. Study of the KNO3–LiNO3 and KNO3–NaNO3–LiNO3 eutectics as phase change materials for thermal storage in a low-temperature solar power plant, *Solar Energy*, 95:155–169. https://doi.org/10.1016/j.solener.2013.06.008

Rosenthal, M W, 2010. An Account of Oak Ridge National Laboratory's Thirteen Nuclear Reactors. Oak Ridge National Laboratories Report ORNL/TM-2009/181. Available at: https://info.ornl.gov/sites/publications/Files/Pub20808.pdf

Serrano-López, R, Fradera, J and Cuesta-López, S, 2013. Molten salts database for energy applications, *Chemical Engineering and Processing: Process Intensification*, 73:87–102. https://doi.org/10.1016/j.cep.2013.07.008

Shrotri, V and Muhmood, L, 2020. Application of geometric models for calculation of viscosity and density of LiNO3 and CsNO3 based ternary nitrate salt systems, *CALPHAD*, 68:101749. https://doi.org/10.1016/j.calphad.2020.101749

Sohal, M S, Ebner, M A, Sabharwall, P and Sharpe, P, 2010. Engineering Database of Liquid Salt Thermophysical and Thermochemical Properties. United States. doi.org/10.2172/980801.

Srivastva, U, Malhotra, R K and Kaushik, S C, 2017. Review of heat transport properties of solar heat transfer fluids, *J Therm Anal Calorim*. https://doi.org/10.1007/s10973-017-6441-y

Tian, Y and Zhao, C Y, 2013. A review of solar collectors and thermal energy storage in solar thermal applications, *Appl Energy*, 104:538–553. https://doi.org/10.1016/j.apenergy.2012.11.051

Trent, M C, Goods, S H and Bradshaw, R W, 2016. Comparison of corrosion performance of grade 316 and grade 347H stainless steels in molten nitrate salt, in *Proceedings of the AIP Conference* (American Institute of Physics Inc). https://doi.org/10.1063/1.4949258

Vignarooban, K, Xu, X, Arvay, A, Hsu, K and Kannan, A M, 2015. Heat transfer fluids for concentrating solar power systems – A review, *Appl Energy*, 146:383–396. https://doi.org/10.1016/j.apenergy.2015.01.125

Zhai, W, Yang, B, Li, M, Li, S, Xin, M, Zhang, S and Huang, G, 2017. Study on corrosion of metal materials in nitrate molten salts, in *Proceedings of the AIP Conference* (American Institute of Physics Inc). https://doi.org/10.1063/1.4971898

Zhang, P, Cheng, J, Jin, Y and An, X, 2018a. Evaluation of thermal physical properties of molten nitrate salts with low melting temperature, *Solar Energy Materials and Solar Cells*, 176:36–41. https://doi.org/10.1016/j.solmat.2017.11.011

Zhang, Y, Huang, M, Kan, Y, Liu, L, Dai, X, Zheng, G and Zhang, Z, 2018b. Influencing factors of viscosity measurement by rotational method, *Polym Test*, 70:144–150. https://doi.org/10.1016/j.polymertesting.2018.06.034

Zhao, C Y and Wu, Z G, 2011. Thermal property characterization of a low melting-temperature ternary nitrate salt mixture for thermal energy storage systems, *Solar Energy Materials and Solar Cells*, 95:3341–3346. https://doi.org/10.1016/j.solmat.2011.07.029